Residues Y179 and H101 of a Hydrophobic Patch of Factor VII Are Involved in Activation by Factor Xa†

Jianping Jin,‡,§ Jinli Chang,‡,|| Darrel W. Stafford,‡,⊥ and David L. Straight*,‡

Department of Biology, University of North Carolina at Chapel Hill, Chapel Hill, North Carolina 27599, and Center for Thrombosis and Hemostasis, University of North Carolina at Chapel Hill, Chapel Hill, North Carolina 27599

Received May 15, 2001; Revised Manuscript Received July 23, 2001

ABSTRACT: We studied factor Xa activation of human factor VII in hopes of identifying factor VII residues, not adjacent to the cleavage site, involved in this interaction. We made eight factor VIIs with single mutations (N100A, H101A, D102Q, L144A, R147A, Y179A, D186A, and F256A) and two factor VIIs with multiple mutations [MM3 (L144A/R147A/D186A) and MM4 (N100A/H101A/Y179A/F256A)]. Residues in MM3 have previously been identified as affecting factor X activation, and the residues of MM4 are located at a hydrophobic patch of factor VII on the opposite side of the catalytic domain from those in MM3. Only H101A, Y179A, and MM4 were activated significantly more slowly than the wild type. Results of our kinetic analyses showed that the catalytic efficiency of factor Xa for activation of factor VII was 176- and 234-fold higher than that for H101A andY179A, respectively. All the mutants with measurable activity had affinities for tissue factor similar to those of the wild type. The activated hydrophobic patch residues, except N100A, which is adjacent to one of the catalytic residues, had normal activities toward both a small peptide substrate and factor X. The rest of the activated mutants (except D102Q with no activity) had reduced activities toward the small substrate (except R147A) and factor X. We conclude that factor VII activation by factor Xa and factor VIIa's catalytic interaction with factor X involve different regions in the catalytic domain, and residues H101 and Y179, part of an aromatic hydrophobic patch, are specifically involved in factor Xa activation of factor VII.

Factor VII is a single-chain plasma glycoprotein with a molecular weight of 50 000, which is converted to a two-chain serine protease when cleaved at the Arg152−Ile153 peptide bond (*1*). The N-terminal region (residues 1−152), called the light chain ($M_r \sim 20\,000$), includes a γ-carboxyglutamic acid domain (Gla, residues 1−45) and two epidermal growth factor-like domains, EGF1 (residues 46−86) and EGF2 (residues 87−152). The C-terminal region, residues 153−406 (residues 6−257, chymotrysin numbering), constitutes the proteolytic domain (heavy chain, $M_r \sim 30\,000$). The conversion of factor VII to factor VIIa can be catalyzed in vitro by a number of proteases, including thrombin (*2*), factor Xa (*3*, *4*), factor IXa (*5*, *6*), and factor XIIa (*5*, *7*). Factor VIIa can also activate factor VII in complex with its cofactor, tissue factor, and calcium (autoactivation) (*8*−*12*). Furthermore, factor VII can be activated by trace amounts of factor VIIa with positively charged surfaces, such as an anion-exchange matrix or polylysine (*10*). In terms of physiological significance, however, a study with a variety of potential activators, including thrombin, factor VIIa/tissue factor, factor IXa, factor Xa, and factor XIa, suggested that the membrane-bound factor Xa is most likely the predominant physiological factor VII activator (*13*).

While several studies have identified parts of factor VIIa that interact with factor X and tissue factor (*14*−*24*), little is known about residues on factor VII that are recognized by factor Xa. If, as it appears, so-called exosites are a general feature of substrate recognition by the enzymes involved in blood coagulation (*16*, *25*−*27*), it seems likely that residues other than those near R152 (factor VII numbering) will be important for the factor Xa−factor VII reaction. Factor VIIa residues interacting with factor X may also be involved in factor Xa recognition, since it has been shown that factor Xa is a competitive inhibitor of factor X activation by the tissue factor−factor VIIa complex (*25*). We tested this possibility by mutating residues in regions believed to interact with factor X, including L144, R147, and D186 (*15*) (the residues in the catalytic domain being represented by the chymotrypsin numbering system).

Another region on the surface of the catalytic domain of factor VIIa attracted our attention, as a likely candidate for functional importance. Located on the opposite side of factor VII from the residues interacting with factor X (Figure 1) and not apparently involved in tissue factor binding, this patch consists of several aromatic residues as well as some nonionic polar residues (Table 1). We selected four residues in this area for mutational analysis, one of which (N100) may also be involved in factor X activation (*15*). We selected

† This work was supported by the National Heart Lung and Blood Institute (Grant HL 38973).

* To whom correspondence should be addressed: Department of Biology, University of North Carolina at Chapel Hill, CB 3280, Chapel Hill, NC 27599. Phone: (919) 962-2267. Fax: (919) 962-9266. E-mail: davids@email.unc.edu.

‡ Department of Biology.

§ Present address: Center for Bioinformatics, University of North Carolina at Chapel Hill, Chapel Hill, NC 27599.

|| Present address: Lineberger Cancer Research Center, University of North Carolina at Chapel Hill, Chapel Hill, NC 27599.

⊥ Center for Thrombosis and Hemostasis.

10.1021/bi010990g CCC: $20.00
Published on Web 08/29/2001

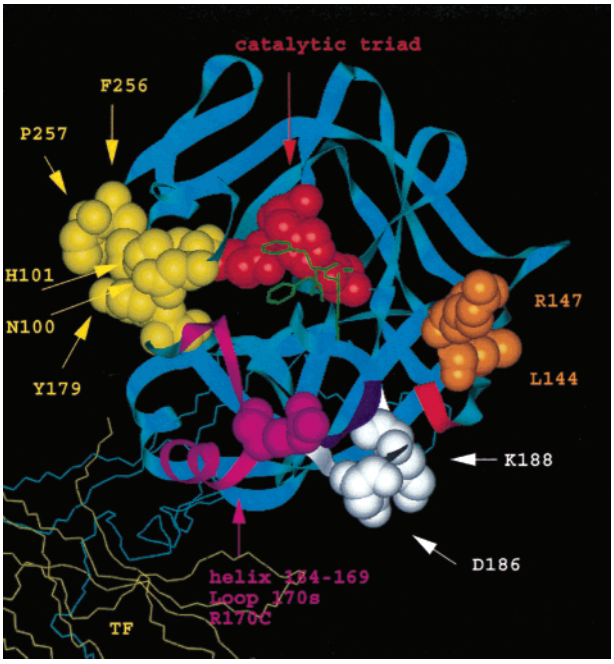

FIGURE 1: Schematic diagram of the catalytic domain of factor VIIa. The diagram represents a side view of the catalytic domain of factor VIIa with tissue factor. The catalytic triad residues are shown in red, and the inhibitor, DFFR, is shown in green. The catalytic cleft runs horizontally across the domain and accommodates the catalytic triad and the inhibitor. The two α-helices of the lower section of the catalytic domain are in contact with tissue factor (yellow thin lines at the bottom). Loop 170s (residues 170−182) is represented by residue 170G in purple, and its location follows one of the two helices (residues 164−169). The residues in white represent loop 1 (residues 185−188) and its neighboring region. The residues in orange represent loop 140s (residues 142−152) and its neighboring region. The residues in yellow represent the surface hydrophobic patch, which is located at the left catalytic cleft end and almost 180° from loop 140s, which may be part of the exosite for factor X binding.

H101, Y179, and F256 for mutation because we thought they would be the least likely to disrupt local conformations. It has been reported that at least one residue (F176S) near this region, when mutated, caused a general conformational change that affects several factor VII functions (*18*). We found that only mutations of the residues, H101 and Y179, in the aromatic hydrophobic patch of factor VII affected factor Xa activation of factor VII. Once activated, however, these mutated factor VIIas displayed normal activities against a small synthetic peptide substrate and factor X, and had affinities for tissue factor similar to that of wild-type factor VIIa.

EXPERIMENTAL PROCEDURES

Materials. Human plasma factor X (without benzamidine) was purchased from Enzyme Research Laboratories, Inc. (South Bend, IN). Agarose-coupled human factor Xa and human factor Xa were from Haematologic Technologies Inc. (Essex Junction, VT). The recombinant tissue factor apoprotein (residues 1−243) was a generous gift from G. Vehar (Genentech, Inc., South San Francisco, CA). Recombinant tick anticoagulant peptide (rTAP)[1] was a generous gift from G. P. Vlasuk (CORVAS International, Inc., San Diego, CA). Chromogenic substrate S-2288 (H-D-isoleucyl-L-prolyl-L-arginine-*p*-nitroaniline dihydrochloride) and S-2222 (*N*-benzoyl-L-isoleucyl-L-glutamylglycyl-L-arginine-*p*-nitroaniline hydrochloride) were purchased from DiaPharma Group, Inc. (West Chester, OH). Oligonucleotides were synthesized by GIBCO BRL Life Technologies (Grand Island, NY). Phosphatidylserine and phosphatidylcholine were purchased from Avanti Polar Lipids (Alabaster, AL).

Table 1: Residue Conservation in an Aromatic Hydrophobic Patch of the Factor VII Catalytic Domain

	91[a]	93[a]	100[a]	101[a]	179[a]	234[a]	237[a]	256[a]
factor VII								
human	P	T	N	H	Y	Y	W	F
rabbit	P	K	D	H	N	Y	W	F
murine	P	K	N	H	N	Y	W	L
bovine	P	Q	D	H	N	Y	W	L
human chymotrypsin	N	K	N	N	A	L	W	−
human trypsin	H	S	N	N	N	Y	W	G
human FIX	H	N	N	H	N	Y	W	−
human FX	H	R	D	F	N	F	W	K
human FVII	P	T	N	H	Y	Y	W	F
human thrombin	H	R	D	R	N	L	W	−
consensus residues	H	R	N		N	Y	W	

[a] Position.

Site-Directed Mutagenesis. We used a human factor VII cDNA as the starting material to create mutant factor VIIs. We performed megaprimer PCR to generate constructs with mutations as previously described (*28*, *29*). Sequences determined by the UNC-CH Sequencing Facility confirmed the presence of the expected mutations and the correct full sequence of all constructs.

Expression and Purification of Recombinant Proteins. The proteins were expressed in HK293 cells and purified essentially as described previously (*30*). However, we eluted the proteins from the Q-Sepharose column with a calcium gradient without benzamidine. The proteins were homogeneous according to sodium dodecyl sulfate−polyacrylamide gel electrophoretic analyses (*31*). Activated protein concentrations were determined by antithrombin III−heparin active site titration (*32*).

Activation of Wild-Type and Mutant Factor VIIs by Factor Xa Coupled to Agarose Beads. For an initial comparison of activation rates, we activated all factor VIIs (0.5 mg/mL) with agarose-coupled factor Xa [10% (w/w) of factor VII] in TNP [20 mM Tris (pH 7.4), 100 mM NaCl, and 0.1% PEG 8000] with 5 mM $CaCl_2$ at ambient temperature. Samples taken between 0 and 90 min were centrifuged to remove the factor Xa resin. We diluted the supernatant with sodium dodecyl sulfate buffer, and analyzed the samples on a 12% polyacrylmide gel (*31*). Protein bands were visualized using silver staining and quantitated by scanning densitom-

[1] Abbreviations: N100A, factor VII in which residue 100 has been changed from N to A; N100Aa, activated N100A (a represents the activated form throughout the paper); H101A, residue H101 replaced with A; D102Q, residue D102 replaced with Q; L144A, residue L144 replaced with A; R147A, residue R147 replaced with A; D186A, residue D186 replaced with A; Y179A, residue Y179 replaced with A; F256A, residue F256 replaced with A; MM3, factor VII with the L144A, R147A, and D186A mutations; MM4, factor VII with the N100A, H101A, Y179A, and F256A mutations; rTAP, recombinant tick anticoagulant peptide; S-2222, *N*-benzoyl-L-isoleucyl-L-glutamylglycyl-L-arginine-*p*-nitroaniline hydrochloride; S-2288, H-D-isoleucyl-L-prolyl-L-arginine-*p*-nitroaniline dihydrochloride; DFFR, D-phenylalanyl-phenylalanylarginyl chloromethyl ketone; PC/PS, 70%/30% phosphatidylcholine/phosphatidylserine vesicles; TNP, 20 mM Tris (pH 7.4), 100 mM NaCl, and 0.1% PEG 8000.

etry. We estimated the half-times for first-order decay using Kaleidagraph software (Synergy Software, Reading, PA).

Kinetic Analysis of Factor VII Activation by Factor Xa. We incubated recombinant wild-type factor VII (0−2 μM) or H101A, Y179A, or MM4 (0−4 μM) with factor Xa (2 nM) in TNP buffer with 5 mM $CaCl_2$ and 20 μM PC/PS vesicles at ambient temperature. After incubation for 2 min (for the wild type) or 10 min (for the mutants), we added rTAP (50 nM, final concentration) to inhibit factor Xa. We determined the optimal concentration of rTAP experimentally. The effective concentration of rTAP that completely inhibited factor Xa (4 nM) activity was 32 nM, and concentrations of rTAP from 10 to 1000 nM have little inhibitory effect on factor VIIa's activity. We measured the amidolytic activity of factor VIIa generated with S2288 (1 mM, final concentration) using a microplate reader (THERMOmax, Molecular Devices).

Assessment of Factor VIIa−Tissue Factor Binding and Amidolytic Activity. We measured the tissue factor affinity of our activated factor VIIs using synthetic substrate S-2288 (1 mM) essentially as previously described (*30*, *33*). We analyzed the data using a quadratic solution to the equilibrium equation as described, and K_d's and maximum cleavage rates were estimated using Kaleidagraph software (Synergy Software).

Measurement of the Kinetics of Factor X Activation. Factor VIIa−tissue factor complexes were formed by incubating factor VIIa (5−10 nM) with relipidated tissue factor (0.5 nM) in TNP buffer with $CaCl_2$ (5 mM) at ambient temperature for 30 min. Relipidated tissue factor was made by incubation of tissue factor with phospholipid vesicles (see vesicle preparation below) in 0.01% (v/v) Tween 80 at 37 °C for 30 min (*33*). Then factor X at final concentrations from 0 to 2 μM was added and incubated at ambient temperature for 2 min before adding 10 mM EDTA to stop the reaction. The amount of factor Xa that was generated was measured using synthetic substrate S-2222. Control experiments with factor X and tissue factor alone showed no significant contamination of factor VII or factor VIIa in the factor X preparation. Velocities were converted to rates of factor Xa generation using a standard curve of factor Xa activity. We analyzed these rates using nonlinear least-squares analyses with Kaleidagraph to determine K_m and k_{cat}.

Preparation of PC/PS Vesicles. Preparation of PC/PS vesicles was carried out as previously described (*34*, *35*) with slight modification. Briefly, we mixed phosphatidylserine and phosphatidylcholine at a 30:70 ratio. The mixture was dried under nitrogen to evaporate the chloroform, suspended in ~3 mL of cyclohexane, and lyophilized. The pellet was suspended in 2 mL of TBS containing 0.1 mM EDTA. The suspension was pushed 10 times through a 0.2 μm filter (sterile Acrodisc, Gelman Sciences) using a 3 mL syringe. The PC/PS vesicles were sealed in a vial under nitrogen and stored at 4 °C for use within 2 weeks.

Molecular Three-Dimensional Graph of Factor VIIa and the Hydrophobic Patch Sequence Alignment. The three-dimensional schematic graph (Figure 1) of factor VIIa was made using Protein Data Bank entry 1dan of the X-ray crystal structure coordinates of the factor VIIa−tissue factor complex using the PSSHOW software (version 2.2, University of California, San Francisco, CA). The alignment of amino acid sequences of trypsin, chymotrypsin, factor VII, factor IX, factor X, and thrombin was performed for the consensus sequence using the program AlignX of the Vector NTI Suite (InforMax Inc., North Bethesda, MD).

Table 2: Half-Time of Factor VII Activation by Factor Xa[a]

substrate (factor VII)	$t_{1/2}$ (min)	substrate (factor VII)	$t_{1/2}$ (min)
wild-type FVII	17	MM4[b]	>90
N100A	30	L144A	12
H101A	82	R147A	10
D102Q	26	D186A	21
Y179A	>90	MM3[c]	21
F256A	17		

[a] The activation of various factor VIIs by solid-phase factor Xa was performed, and the disappearance of the zymogen bands was analyzed as described in Experimental Procedures. The results represent the average of two to four experiments. [b] The multiple mutation (N100A/H101A/Y179A/F256A). [c] The multiple mutation (L144A/R147A/D186A).

Table 3: Kinetic Analysis of H101A and Y179A Activation by Factor Xa[a]

substrate (factor VII)	k_{cat} (s^{-1})	K_m (μM)	k_{cat}/K_m (M^{-1} s^{-1})
wild-type	8.18 ± 1.13	0.35 ± 0.02	2.3×10^7
H101A	0.11 ± 0.02	0.87 ± 0.24	1.3×10^5
Y179A	0.14 ± 0.09	1.42 ± 0.91	9.8×10^4
MM4[b]	nm[c]	nm[c]	nm[c]

[a] Activation of various factor VIIs by soluble factor Xa in the presence of 20 μM PC/PS vesicles was described in Experimental Procedures. Factor Xa was inhibited with rTAP before small substrate was added to measure the amidolytic activity of factor VIIa. The results are representative of three experiments ± the standard deviation. [b] The multiple mutation of factor VII (N100A/H101A/Y179A/F256A). [c] Not measurable.

RESULTS

Activation of Wild-Type and Mutant Factor VII by Agarose-Linked Factor Xa. To estimate the effect of the various mutations on factor VII activation, we assessed the agarose-linked factor Xa-catalyzed disappearance of the factor VII zymogen band on polyacrylamide gels. Results are summarized in Table 2. The activation rates of only three proteins were significantly different from that of normal factor VII: Y179A, H101A, and the multiple mutant containing these two mutations, MM4. The residues previously shown to be possible factor X binding sites in the factor VIIa−tissue factor complex (L144, R147, and D186) and their multiple mutant, MM3, have no effects on factor VII activation. Among the other hydrophobic patch residues, N100A, which affects factor X activation by factor VIIa (*15*) (see results below), was activated slightly more slowly with a $t_{1/2}$ of 30 min and F256A had no effect.

Kinetic Study of Factor VII Activation by Factor Xa. To confirm quantitatively the role of residues H101 and Y179 in factor VII activation by factor Xa, we carried out kinetic analyses. The k_{cat} for activation of factor VII by factor Xa was 8.18 s^{-1} (Table 3), and k_{cat}'s exhibited 74- and 58-fold decreases for H101A and Y179A, respectively. The K_m's for H101A and Y179A were increased by only 2−4-fold over that of wild-type factor VII. The effects on k_{cat} and K_m together resulted in a 176- and 234-fold decrease in the catalytic efficiency (k_{cat}/K_m) of factor Xa for H101A and Y179A, respectively, compared to that of factor VII. The

Table 4: Tissue Factor Affinity and Amidolytic Activity of Various Factor VIIas[a]

factor VIIa	R_{max} ± SD (mOD/min)	K_d ± SD (nM)
wild-type	15.1 ± 0.7	0.4 ± 0.1
N100Aa	3.4 ± 0.3	1.2 ± 0.2
H101Aa	10.4 ± 0.1	0.9 ± 0.1
L144Aa	3.3 ± 0.1	0.2 ± 0.1
R147Aa	18.6 ± 0.9	0.9 ± 0.2
Y179Aa	11.6 ± 0.4	0.5 ± 0.1
D186Aa	1.7 ± 0.1	0.2 ± 0.1
F256Aa	14.7 ± 0.1	1.3 ± 0.1
MM3a[b]	0.2 ± 0.1	0.5 ± 0.3
MM4a[c]	2.7 ± 0.5	1.3 ± 0.5

[a] Various factor VIIas (10 nM) were incubated with increasing amounts of tissue factor (from 0 to 2 μM) for 30 min at ambient temperature. A synthetic substrate, S-2288, was added at a final concentration of 1 mM to measure the activated factor VIIa binding affinity for tissue factor. The results are representative of three experiments. [b] The activated multiple mutation of factor VII (L144A/R147A/D186A). [c] The activated multiple mutation of factor VII (N100A/H101A/Y179A/F256A).

Table 5: Kinetic Parameters for Factor X Activation by Various Factor VIIas[a]

factor VIIa	k_{cat} (s^{-1})	K_m (μM)	k_{cat}/K_m (M^{-1} s^{-1})
wild-type	7.16 ± 0.65	0.21 ± 0.02	3.41×10^7
N100Aa	2.31 ± 0.35	0.15 ± 0.01	1.54×10^7
H101Aa	6.36 ± 0.53	0.17 ± 0.02	3.74×10^7
L144Aa	0.18 ± 0.09	0.13 ± 0.01	0.14×10^7
R147Aa	1.94 ± 0.14	0.18 ± 0.02	1.08×10^7
Y179Aa	6.91 ± 0.43	0.23 ± 0.05	3.00×10^7
D186Aa	1.31 ± 0.11	0.18 ± 0.04	0.73×10^7
F256Aa	6.32 ± 0.10	0.22 ± 0.02	2.87×10^7
MM3a[b]	0.03 ± 0.01	0.25 ± 0.24	1.21×10^5
MM4a[c]	2.35 ± 0.10	0.22 ± 0.02	1.07×10^7

[a] Activation of factor X by various factor VIIas was performed as described in Experimental Procedures. Factor VIIa (10 nM) was incubated with relipidated tissue factor (0.5 nM) in the presence of Ca^{2+} for 30 min. Factor X (from 0 to 2 μM) was added and incubated for 2 min, followed by adding EDTA (10 mM) to stop the reaction. The factor Xa concentration that was generated was measured with S-2288. The results are representative of three or four experiments ± the standard deviation. [b] The activated multiple mutation of factor VII (L144A/R147A/D186A). [c] The activated multiple mutation of factor VII (N100A/H101A/Y179A/F256A).

rate of activation of MM4 was not measurable since it not only is activated slowly but also has low catalytic activity toward the small substrate used for measuring the rate of activation (see below).

Amidolytic Activity, Tissue Factor Affinity, and Factor X Activation of Factor VIIa and Various Mutants. To determine if the effect on activation is the only effect of the mutations we made, we measured the affinity of our mutants for tissue factor using the increase in small substrate activity as a measure of the extent of complex formation. This also serves to tell us whether the mutants have normal activity toward the small substrate. We measured the kinetics of activation of factor X by the various factor VIIa−tissue factor complexes as well.

Results in Table 4 show that H101Aa and Y179Aa have tissue factor affinity and small substrate activity similar to those of wild-type factor VIIa. Mutants previously shown to affect the catalytic activity of factor VIIa (N100A, L144A, and D186A) and the multiple mutants MM4 (containing the N100A mutation) and especially MM3 (containing the L144A and D186A mutations) had reduced activity, but normal affinity for tissue factor. R147Aa, one of the component mutations of MM3, however, exhibited both normal small substrate hydrolysis and tissue factor binding affinity. Consistent with results with mutants H101Aa and Y179Aa, F256Aa (one of the component mutations of MM4) displayed normal small substrate hydrolysis and tissue factor binding affinity as well.

H101Aa and Y179Aa also have normal activity toward factor X (Table 5). F256Aa displayed normal factor X activation as well. As reported earlier, N100Aa has reduced factor Xase activity (*15*) as do the activated forms of L144A, D186A, and their corresponding multiple mutants, MM4a and MM3a. On the other hand, despite having normal small substrate activity, R147Aa had reduced enzymatic activity for factor X activation.

DISCUSSION

Conversion of factor VII to factor VIIa is a crucial step in initiation of blood coagulation (*13*, *36*). Factor Xa appears to be the most effective activator of factor VII (*13*). Krishnaswamy and Betz (*27*) and Baugh et al. (*25*) have shown that in factor Xa and factor VIIa there are so-called exosites on the enzymes that recognize parts of their substrates (prothrombin and factor X, respectively) remote from the cleavage site (P1−P3). Therefore, amino acids in factor VII other than P1−P3 are probably important for recognition by factor Xa.

We investigated the role of certain factor VII residues in this interaction. Our results indicate that at least two residues (H101 and Y179) in an aromatic hydrophobic patch on the catalytic domain of factor VII are specifically involved in factor Xa's activation of factor VII. Factor Xa (on a solid-phase matrix) activates these mutant proteins at least 5-fold slower than it activates wild-type factor VII. Further kinetic characterization of the mutants showed that factor Xa had k_{cat}'s 74- and 58-fold lower for H101A and Y179A, respectively, relative to that of wild-type factor VII. The effects on K_m were more modest, a 2.5- and 4-fold increase for H101A and Y179A, respectively. Like F256Aa, activated H101A and Y179A display normal tissue factor binding affinity and hydrolytic activity toward a small substrate and factor X. This indicates that the slower rate of activation of H101A and Y179A by factor Xa is not caused by a general disruption of the protein conformation by the mutations.

The aromatic hydrophobic patch is a pocketlike structure, with P257, F256, H101, and Y179 at the entry and Y234, W237, and P91 at the bottom and side (Figure 1). We did not test P257, but F256A was activated at a rate similar to that of the wild type. The aromatic hydrophobic patch is close to the active site since N100 and H101 are neighbors to D102, one of the catalytic triad residues. D102Q, the active site residue mutation, showed only a minor effect on factor VII activation ($t_{1/2}$ = 26 min; Table 2). Similarly, the mutation of aromatic hydrophobic patch residues, except N100A, has little effect on the catalytic activity of factor VIIa toward S2288, a small peptide substrate, or factor X.

Mutations of residues (N100, L144, R147, and K186) shown to affect the rate of VIIa's factor X interaction (*15*) (also Table 5) had little (N100) or no effect on factor VII activation by factor Xa. This indicates that the factor X and

factor Xa sites on factor VII(a) are different to the extent they have been tested. This is consistent with the positions of these residues in the three-dimensional structure of factor VIIa. The spatial relationship between the residues previously identified as affecting factor VIIa activation of factor X and those shown in our study to interact with factor Xa is depicted in Figure 1. If we consider the catalytic domain as being divided into two segments by a horizontal axis through the active site, and define the one in contact with tissue factor as the bottom segment, the aromatic hydrophobic patch described in this work is located on the left side of the upper segment. Part of this patch extends through the junction of the two segments. Residues L144 and R147 are on the right side about 180° from our residues. D186 is located in the lower middle of the bottom segment. N100, which has a slight effect on factor VII activation, is, not surprisingly, near the aromatic patch.

According to a recent study (*22*), residue D186 is involved in S1 substrate binding site formation and N-terminal insertion stabilization. Our results are similar to those reported, in that mutation of D186 affects both factor X activation and small substrate hydrolysis (Tables 4 and 5). Unlike D186Aa, R147Aa has normal hydrolytic activity toward the small substrate, S-2288, but reduced activity, compared with that of wild-type factor VIIa, toward factor X activation (Tables 4 and 5). Residue E154 is related to the linkage of the macromolecular substrate binding exosite to the catalytic active site (*21*). Therefore, it appears that loop 140s (residues 142−152) and its neighboring residues contribute to factor X binding. There is evidence that the residues located on the top surface of the upper segment and loop 140s of the catalytic domain are involved in binding to a peptide inhibitor (*23*). Combined with the fact that tissue factor binds to the catalytic domain at the two α-helices located on the bottom segment of factor VII (Figure 1), the evidence suggests the binding sites for the various macromolecules (tissue factor, factor X, and factor Xa) are in different regions and do not overlap.

Others have recently offered evidence that exosites may be a universal feature of coagulation protease−substrate interactions (*25*). If so, residues H101 and Y179 may be the first to be identified as residues that interact with an exosite on a coagulation protease. It will be interesting to see if sequences homologous to this region in other coagulation zymogens are also important for activation. Both the amino acid sequence (Table 1) and the local conformations of this area, as seen in the three-dimensional structures of factors IXa, Xa, and VIIa, are similar, suggesting they may be functionally related as well.

Our kinetic results show the primary effect of both mutations H101A and Y179A is on V_{max} with a modest increase in K_m. Baugh et al. (*25*) showed that the binding constant for the substrate at the active site following binding at the exosite can affect both V_{max} and K_m. Jencks has described how binding energy is converted into a faster catalytic rate (*37*). He proposes that a good substrate and bad substrate may bind with similar affinity, but the good substrate fits into the active site in a conformation more closely resembling the transition state and, therefore, reacts faster. Perhaps our results can be explained in a related way. Mutations of H101 or Y179 cause a slight increase in K_m, suggesting a decrease in substrate affinity. But the actual defect in binding is misalignment of the substrate scissile bond at the active site, which is manifested by a decrease in the catalytic rate.

Thus, we conclude that residues in factor VII's aromatic hydrophobic patch described here are specifically involved in factor VII activation by factor Xa. On the other hand, the region on the other side of the catalytic domain of factor VIIa, which apparently recognizes factor X, is not related to activation by factor Xa. Therefore, the substrate function and enzyme function of factor VII and factor VIIa involve separate surface regions.

ACKNOWLEDGMENT

We thank Dr. George P. Vlasuk (CORVAS International, Inc.) for the gift of recombinant tick anticoagulant peptide and Dr. Gordon Vehar (Genentech, Inc.) for the gift of recombinant tissue factor apoprotein. We thank Dr. D. W. Banner for allowing us to use the factor VII−tissue factor coordinates before they were available at the Protein Data Bank.

REFERENCES

1. Hagen, F. S., Gray, C. L., O'Hara, P., Grant, F. J., Saari, G. C., Woodbury, R. G., Hart, C. E., Insley, M., Kisiel, W., and Kurachi, K. (1986) *Proc. Natl. Acad. Sci. U.S.A. 83*, 2412−6.
2. Radcliffe, R., and Nemerson, Y. (1975) *J. Biol. Chem. 250*, 388−95.
3. Radcliffe, R., and Nemerson, Y. (1976) *J. Biol. Chem. 251*, 4749−802.
4. Rao, L. V., Bajaj, S. P., and Rapaport, S. I. (1985) *Blood 65*, 218−26.
5. Seligsohn, U., Osterud, B., Brown, S. F., Griffin, J. H., and Rapaport, S. I. (1979) *J. Clin. Invest. 64*, 1056−65.
6. Wildgoose, P., and Kisiel, W. (1989) *Blood 73*, 1888−95.
7. Kisiel, W., Fujikawa, K., and Davie, E. W. (1977) *Biochemistry 16*, 4189−94.
8. Nakagaki, T., Foster, D. C., Berkner, K. L., and Kisiel, W. (1991) *Biochemistry 30*, 10819−24.
9. Nemerson, Y., and Esnouf, M. P. (1973) *Proc. Natl. Acad. Sci. U.S.A. 70*, 310−4.
10. Pedersen, A. H., Lund-Hansen, T., Bisgaard-Frantzen, H., Olsen, F., and Petersen, L. C. (1989) *Biochemistry 28*, 9331−6.
11. Ruf, W., Miles, D. J., Rehemtulla, A., and Edgington, T. S. (1992) *J. Biol. Chem. 267*, 22206−10.
12. Neuenschwander, P. F., Fiore, M. M., and Morrissey, J. H. (1993) *J. Biol. Chem. 268*, 21489−92.
13. Butenas, S., and Mann, K. G. (1996) *Biochemistry 35*, 1904−10.
14. Neuenschwander, P. F., and Morrissey, J. H. (1995) *Biochemistry 34*, 8701−7.
15. Dickinson, C. D., Kelly, C. R., and Ruf, W. (1996) *Proc. Natl. Acad. Sci. U.S.A. 93*, 14379−84.
16. Dickinson, C. D., Shobe, J., and Ruf, W. (1998) *J. Mol. Biol. 277*, 959−71.
17. Banner, D. W., D'Arcy, A., Chene, C., Winkler, F. K., Guha, A., Konigsberg, W. H., Nemerson, Y., and Kirchhofer, D. (1996) *Nature 380*, 41−6.
18. Bharadwaj, D., Iino, M., Kontoyianni, M., Smith, K. J., Foster, D. C., and Kisiel, W. (1996) *J. Biol. Chem. 271*, 30685−91.
19. Matsushita, T., Kojima, T., Emi, N., Takahashi, I., and Saito, H. (1994) *J. Biol. Chem. 269*, 7355−63.
20. O'Brien, D. P., Gale, K. M., Anderson, J. S., McVey, J. H., Miller, G. J., Meade, T. W., and Tuddenham, E. G. (1991) *Blood 78*, 132−40.
21. Shobe, J., Dickinson, C. D., and Ruf, W. (1999) *Biochemistry 38*, 2745−51.
22. Petrovan, R. J., and Ruf, W. (2000) *Biochemistry 39*, 14457−63.

23. Dennis, M. S., Eigenbrot, C., Skelton, N. J., Ultsch, M. H., Santell, L., Dwyer, M. A., O'Connell, M. P., and Lazarus, R. A. (2000) *Nature 404*, 465−70.
24. Ruf, W. (1994) *Biochemistry 33*, 11631−6.
25. Baugh, R. J., Dickinson, C. D., Ruf, W., and Krishnaswamy, S. (2000) *J. Biol. Chem. 275*, 28826−33.
26. Shobe, J., Dickinson, C. D., Edgington, T. S., and Ruf, W. (1999) *J. Biol. Chem. 274*, 24171−5.
27. Krishnaswamy, S., and Betz, A. (1997) *Biochemistry 36*, 12080−6.
28. Datta, A. K. (1995) *Nucleic Acids Res. 23*, 4530−1.
29. Sarkar, G., and Sommer, S. S. (1990) *BioTechniques 8*, 404−7.
30. Jin, J., Chang, J., Chang, J. Y., Kelley, R. F., Stafford, D. W., and Straight, D. L. (1999) *Biochemistry 38*, 1185−92.
31. Laemmli, U. K. (1970) *Nature 227*, 680−5.
32. Griffith, M. J., Breitkreutz, L., Trapp, H., Briet, E., Noyes, C. M., Lundblad, R. L., and Roberts, H. R. (1985) *J. Clin. Invest. 75*, 4−10.
33. Krishnaswamy, S. (1992) *J. Biol. Chem. 267*, 23696−706.
34. Mayer, L. D., Hope, M. J., and Cullis, P. R. (1986) *Biochim. Biophys. Acta 858*, 161−8.
35. Hope, M. J., Bally, M. B., Webb, G., and Cullis, P. R. (1985) *Biochim. Biophys. Acta 812*, 55−65.
36. Roberts, H. R., and Tabares, A. H. (1995) Overview of the Coagulation Reactions, in *Molecular Basis of Thrombosis and Hemostasis* (High, K. A., and Roberts, H. R., Eds.) pp 36, Marcel Dekker, New York.
37. Jencks, W. P. (1987) in *Catalysis in Chemistry and Enzymology*, pp 701−3, Dover Publications, New York.

BI010990G